Journal of Zhejiang University-SCIENCE A (Applied Physics & Engineering)
ISSN 1673-565X (Print); ISSN 1862-1775 (Online)
www.zju.edu.cn/jzus; www.springerlink.com
E-mail: jzus@zju.edu.cn

The role of humic acid in stabilizing fullerene (C_{60}) suspensions

Lu-qing ZHANG[1], Yu-kun ZHANG[1], Xiu-chun LIN[1,3], Kun YANG[1,2], Dao-hui LIN[†‡1,2]

([1]*Department of Environmental Science, Zhejiang University, Hangzhou 310058, China*)

([2]*Zhejiang Provincial Key Laboratory of Organic Pollution Process and Control, Hangzhou 310058, China*)

([3]*College of Environmental and Biological Engineering, Putian University, Putian 351100, China*)

[†]E-mail: lindaohui@zju.edu.cn

Received Apr. 30, 2014; Revision accepted June 13, 2014; Crosschecked July 20, 2014

Abstract: Natural organic matter (NOM) has a profound effect on the colloidal stability of discharged C_{60} nanoparticles in the water environment, which influences the environmental behaviors and risks of C_{60} and therefore merits more specific studies. This study investigates the effects of humic acid (HA), as a model NOM, on the aqueous stabilization of C_{60} powder and the colloidal stability of a previously suspended C_{60} suspension (aqu/nC_{60}) with variations of pH values and ionic strengths. Our results reveal that HA could disperse C_{60} powder in water to some degree, but was unable to stably suspend them. The aqu/nC_{60} could remain stable at pH>4 but was destabilized at lower pH values. However, the colloidal stability of aqu/nC_{60} in the presence of HA was insensitive to pH 3–11, owing to the adsorption of HA onto nC_{60} and the increased electrosteric repulsions among nC_{60} aggregates. The colloidal stability of aqu/nC_{60}, with and without HA, decreased as we increased the valence and concentration of the added cations. HA was found to mitigate the destabilization effect of Na^+ on the colloidal stability of aqu/nC_{60} by increasing the critical coagulation concentration (CCC) of Na^+, while HA lowered the CCCs of Ca^{2+} and La^{3+} probably by the bridging effect of nC_{60} with HA aggregates formed through the intermolecular bridging of the HA macromolecules via cation complexation at high concentrations of cations with high valences.

Key words: Fullerene, Humic acid, Colloidal stability, Natural organic matter, Nanomaterial
doi:10.1631/jzus.A1400115 **Document code:** A **CLC number:** X52

1 Introduction

Fullerene C_{60} nanoparticles have triggered much attention by their unique physicochemical, electrical, and mechanical properties, which enable their numerous potential applications in electronics (Zhang *et al*., 2013), biomedicine (Colvin, 2003; Nakamura and Isobe, 2003), cosmetics (Takada *et al*., 2006), etc. C_{60} is inevitably released into the aquatic environment with its widespread production and usage (van Wezel *et al*., 2011), and may thus threaten aquatic organisms and human health as well through food chains (Nel *et al*., 2006; Oberdörster *et al*., 2006; Britto *et al*., 2012).

Once released into the water environment, the hydrophobic C_{60} will be presented as aggregates (nC_{60}). Ubiquitous natural organic matter (NOM), such as humic acid (HA), is likely to interact with the discharged nC_{60} and influence the aggregation/dispersion behavior and ecotoxicity of nC_{60} (Bhatt and Tripathi, 2011; Kim *et al*., 2012). Therefore, it is essential to take into account the interactions between NOM and nC_{60} when elucidating the behavior of nC_{60} in natural water bodies.

Several studies have investigated the interaction between NOM and nC_{60} and the effect of NOM on the aggregation/dispersion behavior of nC_{60}. Xie *et al.* (2008) observed significant changes in the aggregate

‡ Corresponding author
* Project supported by the National Natural Science Foundation of China (No. 21337004), the National Basic Research Program (973) of China (No. 2014CB441104), the Zhejiang Provincial Natural Science Foundation of China (No. LR12B07001), the Specialized Research Fund for the Doctoral Program of Higher Education (SRFDP) (No. 20130101110132), the Fujian Provincial Natural Science Foundation of China (No. 2014J01053), and the Fundamental Research Funds for the Central Universities (No. 2014FZA6009), China

size and morphology of nC_{60} with the addition of NOM. Li *et al.* (2009) revealed that NOM could effectively stabilize nC_{60} in the aqueous phase and nC_{60} nanoparticles may have been chemically modified under illumination. Mashayekhi *et al.* (2012) attributed the increased stability of nC_{60} to the transformation of surface properties through the HA adsorption. The adsorption of HA can increase electrostatic and steric repulsions among nC_{60} aggregates, and thus facilitate dispersion and stabilization of nC_{60} in water (Chen and Elimelech, 2007; Mashayekhi *et al*., 2012; Zhang *et al*., 2013). Moreover, environmental conditions (e.g., water quality parameters) may have profound effects on the interaction between HA and nC_{60} (Isaacson and Bouchard, 2010; Qu *et al*., 2010; Yang *et al*., 2013), which has not been well examined. Chen and Elimelech (2007) found that HA could increase the C_{60} nanoparticle stability in NaCl or $MgCl_2$ electrolytes, but HA enhanced the aggregation at high concentrations of $CaCl_2$. Therefore, water quality parameters, such as ionic strength and pH, are likely to have significant effects on the colloidal stability of C_{60} in the presence of HA, which merit further investigations.

This work is aimed to study the capabilities of HA in dispersing and stabilizing C_{60} powder in water and in maintaining the colloidal stability of nC_{60} suspension (aqu/nC_{60}) as affected by variations of pH and ionic strength. The changes of zeta potentials and hydrodynamic sizes of the C_{60} powder and aqu/nC_{60} under different pH values and the impact of ionic strength on the aggregation kinetics of the aqu/nC_{60} in the absence and presence of HA were specifically examined.

2 Materials and methods

2.1 Preparation and characterization of HA

HA was purchased from Sigma-Aldrich. HA was purified before use and was characterized following the procedures detailed in Lin *et al*. (2012a; 2012b). HA of 500 mg was dissolved in 10 ml 1 mol/L NaOH solution, and adjusted to pH 7.0 using 1 mol/L HCl. The supernatant was obtained by centrifugation at 3000 r/min for 15 min, and then was diluted to 1 L using ultra-pure water and used as the stock HA solution (500 mg/L). NaN_3 (200 mg/L) was added to prevent HA from microbial interference. The HA solution was scanned with an ultraviolet (UV) spectrophotometer (SHIMADZU, UV-2450, Japan).

2.2 Preparation and characterization of aqu/nC_{60}

C_{60} powder was purchased from Nanjing XFNANO Materials Tech Co., Ltd., China. The elemental contents were measured using an elemental analyzer (Vario ELIII, Germany). Aqueous suspension of C_{60} was prepared following a solvent exchange procedure modified from previous works (Deguchi *et al*., 2001; Chen and Elimelech, 2006; Kim *et al*., 2010). C_{60} powder (120 mg) was dispersed in 60 ml of high-performance liquid chromatography (HPLC)-grade toluene by stirring for several hours, forming a clear dark purple mixture. The mixture was then added into ultra-pure water at a volume ratio of 1:15, resulting in two distinct phases. The resultant mixture was sonicated with a sonifier cell disrupter (KBS-150, Kunshan, China) for more than 4 h, allowing for the evaporation of toluene. The stabilized C_{60} suspension (aqu/nC_{60}) was obtained by centrifugation at 2000 r/min for 15 min, and then stored at room temperature in the dark. The morphology and aggregate size of the aqu/nC_{60} were examined with a transmission electron microscope (TEM; JEM-1230, JEOL, Japan). The hydrodynamic size and zeta potential were determined using a Zetasizer (Nano ZS90, Malvern Instruments, UK) at 25 °C (Tian *et al.*, 2010). The aqu/C_{60} suspension was also scanned using the UV spectrophotometer.

2.3 Suspension experiment

A suspension experiment was performed to study the effect of HA on the aqueous stabilization of C_{60} powder. C_{60} powder (10 mg) was added into 20 ml of HA solutions (pH 7.0, 10 mg/L of NaCl) with initial HA concentrations of 0, 5, 10, 20, and 40 mg/L. The mixtures were sonicated (240 W, 40 KHz) for 1 h and were subsequently kept in a thermostat shaker (150 r/min, 25 °C) for 1 d. The zeta potential and hydrodynamic size of the samples were measured right after the shaking process with the Zetasizer at 25 °C. Each concentration was run in triplicate. The absorbance at 800 nm (UV800) was considered to be capable of quantifying the stabilized multi-walled carbon nanotubes (MWCNTs) (Lin *et al*., 2010; 2012a). Similarly, UV800 of the C_{60}

suspension was in a positive correlation with the concentration of suspended C_{60} determined by a total organic carbon (TOC) analyzer (SHIMADZU, TOC-VCPH, Japan), and the HA solution had no absorbance at 800 nm (Fig. 1). Therefore, the UV800 of the supernatant of the C_{60}-HA suspension after settling for 0–2 d was used to measure the stability of the nC_{60} suspensions in the presence of different concentrations of HA.

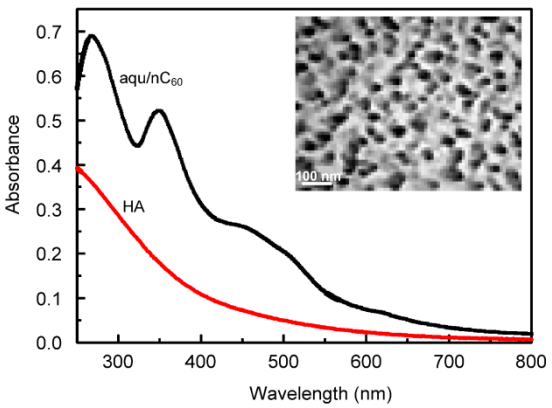

Fig. 1 TEM image of the aqu/nC_{60} and UV-vis absorbance spectra of the aqu/nC_{60} (8 mg/L) and HA (10 mg/L)

2.4 Effect of pH on stability of aqu/nC_{60} with and without HA

The stock suspension of aqu/nC_{60} (10 ml) was added into 22-ml glass vials containing 10 ml of ultrapure water or 20 mg/L HA with 20 mg/L NaCl. The pH values of the suspensions were then adjusted to 3.0–11.0 with several drops of 1 mol/L NaOH or HCl solutions. The mixtures were equilibrated (150 r/min) for 1 d, and then their zeta potentials, hydrodynamic sizes, and final pH values were measured. Each pH value was run in triplicate.

2.5 Aggregation kinetics of aqu/nC_{60} with and without HA

Aggregation kinetics of the aqu/nC_{60} in the presence and absence of HA were investigated under various ionic strengths using a time-resolved dynamic light scattering (DLS) technique. A portion of the stock aqu/nC_{60} of pH 7.0 with or without 10 mg/L HA was added into a polystyrene measurement cell and the hydrodynamic sizes were recorded by the Zetasizer at an interval of 1 min for 30 min at 25 °C. Various ionic strengths were obtained by mixing 0.5 ml of NaCl, $CaCl_2$, or $LaCl_3$ solutions of different concentrations into the cells containing aqu/nC_{60} prior to the hydrodynamic size measurements. At the early stage of aggregation, the initial aggregation rate of the aqu/nC_{60} can be expressed as

$$\left(\frac{D_{\mathrm{h}}(t)}{\mathrm{d}t}\right)_{t\to 0} \propto k_{11}N_0, \tag{1}$$

where $D_{\mathrm{h}}(t)$ is the hydrodynamic size (nm) of nC_{60} at time t, N_0 is the initial particle concentration (mg/L), and k_{11} is the initial aggregation rate constant (Chen and Elimelech, 2006; Chen *et al*., 2006). The initial rate of increase in $D_{\mathrm{h}}(t)$ is obtained by determining the initial slope up to the point where the hydrodynamic size reaches $1.25D_{\mathrm{h}}(0)$.

The attachment efficiency (α) under different ionic strengths was calculated to quantify the aggregation kinetics of the aqu/nC_{60}:

$$\alpha = \frac{k_{11}}{(k_{11})_{\mathrm{fast}}} = \frac{\dfrac{1}{N_0}\left(\dfrac{\mathrm{d}D_h(t)}{\mathrm{d}t}\right)_{t\to 0}}{\dfrac{1}{(N_0)_{\mathrm{fast}}}\left(\dfrac{\mathrm{d}D_h(t)}{\mathrm{d}t}\right)_{t\to 0,\ \mathrm{fast}}}, \tag{2}$$

where $(k_{11})_{\mathrm{fast}}$ refers to k_{11} in the diffusion controlled regime (Mashayekhi *et al*., 2012).

3 Results and discussion

3.1 Characteristics of aqu/nC_{60} and HA

Selected properties of the C_{60} powder and HA are listed in Table 1. The aggregate size of aqu/nC_{60} as determined using TEM was (34.8±5.9) nm (Fig. 1). The transparent yellow aqu/nC_{60} remained stable for several months during and after the experiments. The concentration of the stock aqu/nC_{60} was 8.0 mg C/L with the zeta potential of −40.8 mV, hydrodynamic size of 172 nm, and pH value of 7.0. Fig. 1 shows the UV-vis absorbance spectrum of the aqu/nC_{60}. The aqu/nC_{60} had absorption peaks at 269 and 350 nm as well as a broad band between 410 and 550 nm, which were identified to be characteristics of nC_{60} suspension as previously reported (Hyung and Kim, 2009; Hwang and Li, 2010; Navarro *et al*., 2013).

3.2 Effect of HA on aqueous stabilization of C_{60}

Fig. 2 shows the changes of zeta potential, hydro-dynamic size, and UV800 of the C_{60} powder sonicated in water against a concentration of HA. The zeta potentials of the C_{60} powder in the presence of 0–40 mg/L HA were all lower than –50 mV, and the electronegativity initially increased with increasing the HA concentration and then leveled off at about –65 mV (Fig. 2a). The greater electronegativity of the C_{60} powder in the presence of HA indicated a greater electrostatic repulsion among the C_{60} particles, which was evidenced by the smaller hydrodynamic sizes in the HA solutions (Fig. 2a). The hydrodynamic size of the C_{60} powder was (953±145) nm in the absence of HA, which however decreased to (516±31) nm in the presence of 40 mg/L HA, suggesting that HA could disperse the C_{60} powder to some degree in water.

The increased electrostatic repulsion between C_{60} aggregates accompanied by decreased hydrodynamic size with increasing HA concentrations led to the enhanced aqueous suspension of C_{60} in the HA solutions, which was confirmed by the increased UV800 of the C_{60} powder in the HA solutions. UV800 of the C_{60}-HA suspension was positively correlated with the HA concentration after settling for 0−2 d, which was in accordance with the changes of zeta potential and hydrodynamic size against the HA concentration (Fig. 2b). However, the UV800 of the C_{60}-HA suspensions decreased with increasing settling time. After settling for 2 d, all of the C_{60}-HA suspensions became transparent, suggesting the severe agglomeration and precipitation of the C_{60} aggregates. The above result implies that after being discharged, the hydrophobic C_{60} powder could hardly be dispersed and stabilized in the water environment even in the presence of HA.

3.3 Effect of pH on aqueous stability of aqu/nC_{60} with and without HA

The stability of aqu/nC_{60} in the absence and presence of HA was investigated under various pH values. Dramatic increases in electronegativity of the aqu/nC_{60} with and without HA were observed as pH increased from 3 to 6, while the increases leveled off over pH 6 (Fig. 3). This suggests that the neutralization reaction between H^+ and the acidic surfaces of aqu/nC_{60} occurred at low pH (Yang *et al.*, 2013), thereby reducing the electronegativity and electrostatic repulsion among the nC_{60} aggregates and consequently causing the aggregation and destabilization of the aqu/nC_{60} in the absence of HA. The aqu/nC_{60} had a lower zeta potential in the presence of 10 mg/L HA, and the differences between the zeta potentials

Table 1 Selected properties of C_{60} and HA

Material	Elemental content (%)				Ash (%)	Acidic site (mmol/g)		
	C	H	N	O		Total	–COOH	Phenolic –OH
C_{60}	99.70	0.01						
HA	59.90	3.94	1.50	31.50	3.20	7.15	4.25	2.90

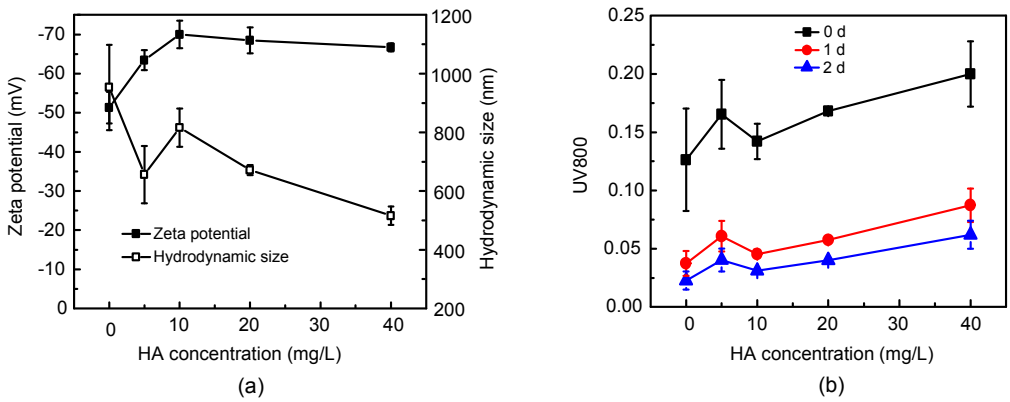

Fig. 2 Variations of zeta potential and hydrodynamic size (a) and UV-vis absorbance at 800 nm (UV800) (b) of C_{60} powder sonicated in water after settling for 0–2 d with HA

Data are presented as mean±standard deviation, n=3

with and without HA became more significant under acidic conditions (pH<6). HA could be adsorbed by the nC_{60} aggregates (Mashayekhi *et al*., 2012), and the dissociation of –COOH and phenolic –OH groups of the surface-bound HA (Table 1) could impart negative charges on the nC_{60} aggregates, causing the difference in the zeta potential of the aqu/nC_{60} with and without HA.

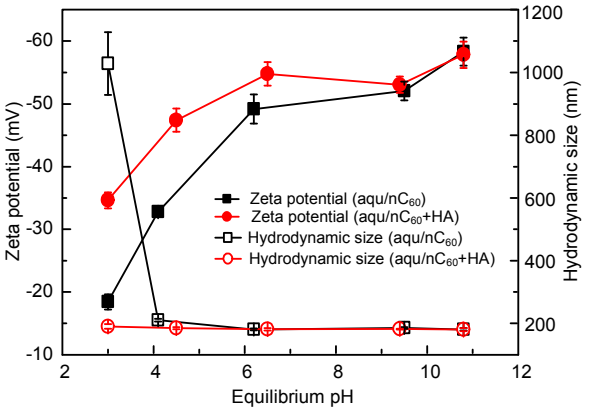

Fig. 3 Variations of zeta potentials and hydrodynamic sizes of the aqu/nC_{60} with and without HA (10 mg/L)

The aqu/nC_{60} retained its hydrodynamic size of (186±10) nm at pH>4 with and without HA (Fig. 3). The hydrodynamic size of the aqu/nC_{60} in the absence of HA sharply increased to (1028±100) nm at pH=3, whereas it remained largely unchanged in the presence of HA (Fig. 3). The differences in the hydrodynamic size of the aqu/nC_{60} with and without HA at pH=3 could be explained by the differences in the zeta potential. At pH=3, the zeta potential of the aqu/nC_{60} increased to (−18±1) mV in the absence of HA while it remained lower than −30 mV in the presence of HA (Fig. 3). Colloids with absolute zeta potential >30 mV are considered to have strong electrostatic repulsions and tend to remain dispersed, while with the absolute zeta potential lower than 30 mV, they are prone to aggregation and destabilization due to the weak electrostatic repulsions among them (Lin *et al*., 2009; 2012a). The adsorbed HA could mitigate the neutralization reaction between H^+ and the acidic surfaces of the aqu/nC_{60}, preventing the nC_{60} from aggregation, owing to the decreased electrostatic repulsion at low pH values. Moreover, the adsorbed HA could also enhance the aqueous stability of aqu/nC_{60} via the increased steric hindrance among the nC_{60} aggregates. From the above results, we can see that the aqu/nC_{60} would remain stabilized in the water environment with broad pH values, but would be subject to aggregation and destabilization at extremely low pH values; the coexisting HA is likely to help to stabilize the aqu/nC_{60}, especially at low pH values.

3.4 Effect of ionic strength on aqueous stability of aqu/nC_{60} with and without HA

3.4.1 Aggregation kinetics of the aqu/nC_{60} in the absence of HA

Aggregation of the aqu/nC_{60} occurred after the addition of various concentrations of the electrolytes as evidenced by the increase in its hydrodynamic size (Fig. 4). The cations at high concentrations immediately increased the aggregate size after their addition to the aqu/nC_{60}. Fig. 4a shows the increasing of the aggregation rate of the aqu/nC_{60} by increasing Na^+ concentration from 50 to 400 mmol/L during 30 min. The hydrodynamic size remained constant when 50 mmol/L Na^+ was added. But the aggregation rate markedly increased with the concentration of Na^+ increasing from 50 to 150 mmol/L, and then remained steady with further addition of Na^+. The attachment efficiencies (α) of the aqu/nC_{60} at each Na^+ concentration were calculated according to Eq. (2) (Fig. 5a). The increase in Na^+ concentration could screen the surface charge of nC_{60}, reduce the electrostatic energy barrier, and subsequently lead to the fast aggregation in the reaction controlled regime where α linearly increased with the increasing Na^+ concentration. However, once the electrolyte concentration was beyond the critical coagulation concentration (CCC), the energy barrier was completely eliminated and the diffusion controlled aggregation began. Under the diffusion controlled regime, α no longer responded to the increasing Na^+ concentration. Based on the data in Fig. 5a, the CCC, the intersection of the reaction and diffusion controlled regimes, was determined to be 142 mmol/L for Na^+.

The DLS measurement was also applied to study the aggregation kinetics of aqu/nC_{60} in the presence of Ca^{2+} and La^{3+}. The increases in the hydrodynamic size with time were observed starting at 3 and 0.07 mmol/L of Ca^{2+} (Fig. 4c) and La^{2+} (Fig. 4e), respectively, revealing that much lower concentrations of the cations with higher valence were needed to destabilize the aqu/nC_{60}. This is because cations

with higher valence have much higher capability of eliminating the energy barrier between the dispersed nanoparticles and thereby promoting the aggregation (Chen *et al*., 2006). The increase in aggregation rate of the aqu/nC_{60} leveled off (i.e., α=1) with the concentrations of Ca^{2+} and La^{3+} over 5 and 0.1 mmol/L, respectively. Figs. 5b and 5c show variations of α of the aqu/nC_{60} with the concentrations of Ca^{2+} and La^{3+}, where their CCCs were calculated to be 5.30 and 0.110 mmol/L, respectively. The ratio of CCCs of the three electrolytes NaCl:$CaCl_2$:$AlCl_3$ was 140:5.30:0.110 (i.e., $1^{-4.78}$:$2^{-4.78}$:$3^{-4.78}$) (Fig. 5d), which was close to the ratio indicated by the Schulze-Hardy rule (i.e., 1^{-6}:2^{-6}:3^{-6}) (Li and Huang, 2010).

Our CCC of NaCl is comparably higher than that determined by Chen and Elimelech (2006) for fullerene nanoparticles synthesized using the same technique (120 mmol/L). Their reported CCC of $CaCl_2$ was 4.8 mmol/L, which was close to our obtained result. It was noteworthy that the CCC values were quite similar, regardless of the 10 times higher suspension concentration which we employed, implying that the initial concentration of aqu/nC_{60} may play an insignificant role in its aggregation.

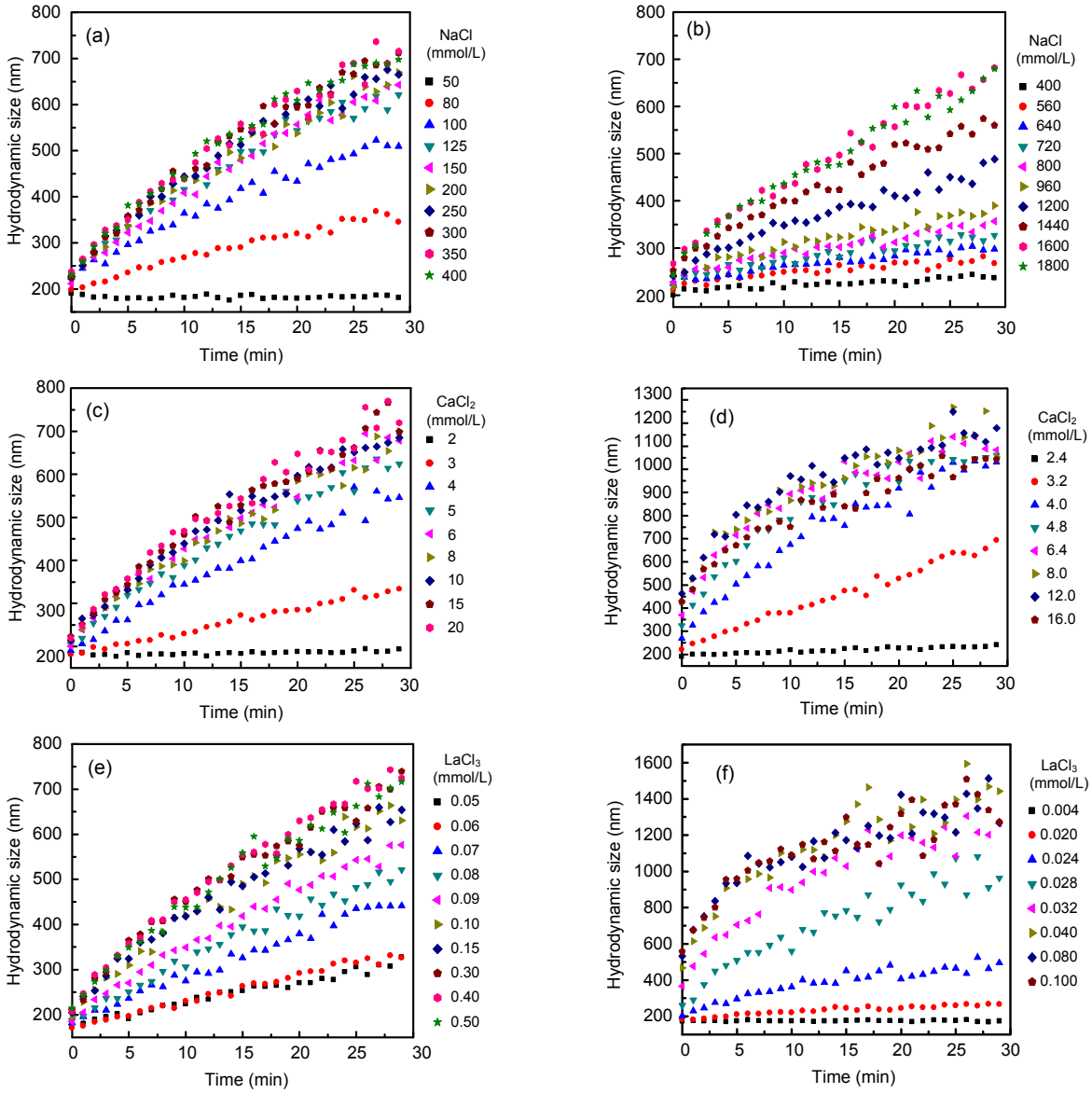

Fig. 4 Aggregation kinetics of the aqu/nC_{60} at different concentrations of NaCl (a, b), $CaCl_2$ (c, d), and $LaCl_3$ (e, f) in the absence (a, c, e) and presence (b, d, f) of 10 mg/L HA

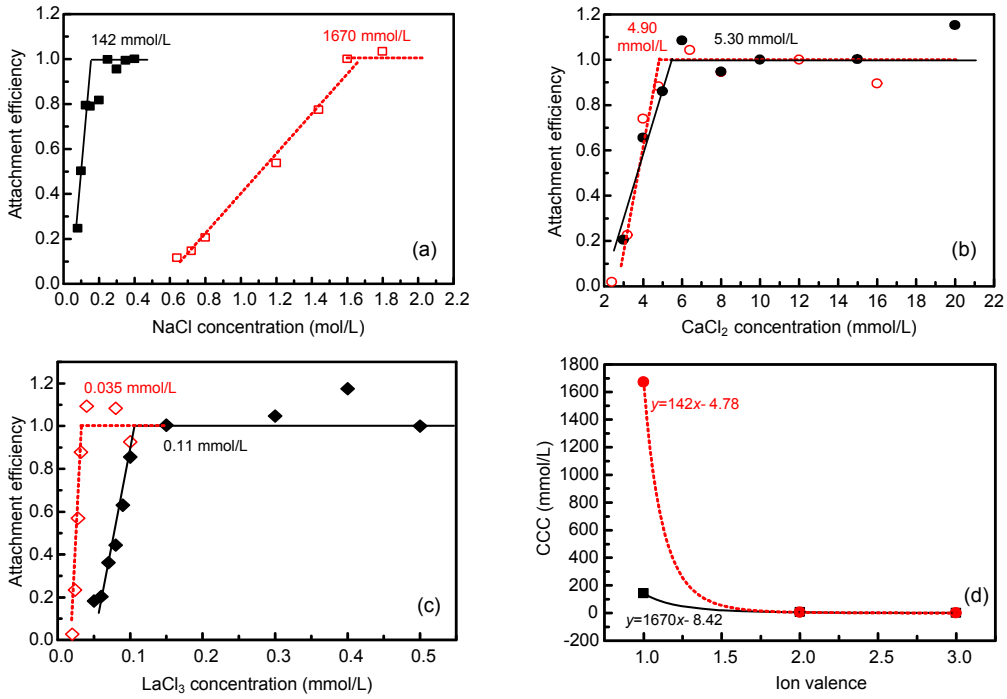

Fig. 5 Attachment efficiencies of the aqu/nC_{60} at different concentrations of NaCl (a), $CaCl_2$ (b), $LaCl_3$ (c), and the relationship between CCCs and cation valences (d) in the absence (solid lines) and presence (dash lines) of 10 mg/L HA

The CCCs of the eletrolytes were marked in the figures

3.4.2 Aggregation of aqu/nC_{60} in the presence of HA

The effects of HA on the aggregation rate of aqu/nC_{60} at different concentrations of NaCl, $CaCl_2$, and $LaCl_3$ are shown in Figs. 4b, 4d, and 4f, respectively. aqu/nC_{60} started to aggregate with the hydrodynamic size increasing with time at Na^+ concentrations higher than 600 mmol/L and did not reach its maximum aggregation rate until 1670 mmol/L (CCC) of NaCl (Fig. 5a). Clearly, the presence of HA effectively prevented the aqu/nC_{60} from homoaggregation and forming bigger aggregates as affected by NaCl. This was in accordance with the result of a previous study that NOM increased the stability of nC_{60} suspension (Duncan *et al*., 2008). It was supposed that the adsorption of NOM including HA on the nC_{60} aggregates could increase electrosteric repulsions and thereby enhance stabilization of the nC_{60} suspension (Chen and Elimelech, 2007). Environmental concentrations of Na^+ are generally much lower than 1670 mmol/L, therefore the Na^+ effect on the stability of aqu/nC_{60} could be ignored in the presence of 10 mg/L HA.

The aggregation rate of aqu/nC_{60} started to increase at 3.2 and 0.02 mmol/L of Ca^{2+} (Fig. 4d) and La^{3+} (Fig. 4f) and the increase leveled off at 4.80 and 0.032 mmol/L of Ca^{2+} (Fig. 5b) and La^{3+} (Fig. 5c), respectively. According to Figs. 5b and 5c, the calculated CCCs were 4.90 and 0.035 mmol/L of Ca^{2+} and La^{3+}, respectively, which were surprisingly lower than their respective CCCs in the absence of HA. The negative effect of HA on the stability of aqu/nC_{60} as affected by Ca^{2+} was also observed by Chen and Elimelech (2007). The accelerated aggregation in the presence HA was attributed to the bridging of nC_{60} by the HA aggregates formed through the intermolecular bridging of HA macromolecules via cation complexation at high concentrations of cations with high valences (Chen and Elimelech, 2007). The ratio of CCCs of the three electrolytes NaCl:$CaCl_2$:$AlCl_3$ in the presence of HA was 1670:4.90:0.035 (i.e., $1^{-8.42}$:$2^{-8.42}$:$3^{-8.42}$) (Fig. 5d), which was also largely comparable to the precipitation by the Schulze-Hardy rule (i.e., 1^{-6}:2^{-6}:3^{-6}) (Li and Huang, 2010) but was different from the ratio in the absence of HA. This differences were owing to the different effects of the HA

on the colloidal stability of the aqu/nC_{60} as affected by the three electrolytes as addressed above.

4 Conclusions

The effects of HA on the aqueous stabilization of C_{60} powder and on the colloidal stability of aqu/nC_{60} as affected by variations of pH and ionic strength were studied. C_{60} powder could be dispersed to some degree but hardly be stably suspended in the presence of HA. Low pH and high ionic strength would affect the colloidal stability of aqu/nC_{60}. Big aggregates formed at pH<4, owing to the screening of surface charges of the aqu/nC_{60} at such low pH. However, the colloidal stability of aqu/nC_{60} in the presence of HA was insensitive to pH 3–11. It was supposed that HA could be adsorbed onto the surfaces of nC_{60} and the surface-bound HA increased the surface electronegativity of the nC_{60}, and thereby mitigated the aggregation through electrosteric repulsion at low pH values. Cation valence and concentration had a profound effect on the destabilization of the aqu/nC_{60}. The CCCs of Na^+, Ca^{2+}, and La^{3+} in the presence and absence of HA were exponentially decreased with the increase in cationic valence. The presence of HA could mitigate the impact of Na^+ on the colloidal stability of aqu/nC_{60}, but enhanced the destabilization effect of Ca^{2+} and La^{3+} on the aqu/C_{60}.

References

Bhatt, I., Tripathi, B.N., 2011. Interaction of engineered nanoparticles with various components of the environment and possible strategies for their risk assessment. *Chemosphere*, **82**(3):308. [doi:10.1016/j.chemosphere.2010.10.011]

Britto, R.S., Garcia, M.L., Rocha, A.M., *et al*., 2012. Effects of carbon nanomaterials fullerene C_{60} and fullerol $C_{60}(OH)_{18–22}$ on gills of fish *Cyprinus carpio* (Cyprinidae) exposed to ultraviolet radiation. *Aquatic Toxicology*, **114-115**:80-87. [doi:10.1016/j.aquatox.2012.02.018]

Chen, K.L., Elimelech, M., 2006. Aggregation and deposition kinetics of fullerene (C_{60}) nanoparticles. *Langmuir*, **22**(26):10994-11001. [doi:10.1021/la062072v]

Chen, K.L., Elimelech, M., 2007. Influence of humic acid on the aggregation kinetics of fullerene (C_{60}) nanoparticles in monovalent and divalent electrolyte solutions. *Journal of Colloid and Interface Science*, **309**(1):126-134. [doi:10.1016/j.jcis.2007.01.074]

Chen, K.L., Mylon, S.E., Elimelech, M., 2006. Aggregation kinetics of alginate-coated hematite nanoparticles in monovalent and divalent electrolytes. *Environmental Science & Technology*, **40**(5):1516-1523. [doi:10.1021/es0518068]

Colvin, V.L., 2003. The potential environmental impact of engineered nanomaterials. *Nature Biotechnology*, **21**(10):1166-1170. [doi:10.1038/nbt875]

Deguchi, S., Alargova, R.G., Tsujii, K., 2001. Stable dispersions of fullerenes, C_{60} and C_{70}, in water. Preparation and characterization. *Langmuir*, **17**(19):6013-6017. [doi:10.1021/la010651o]

Duncan, L.K., Jinschek, J.R., Vikesland, P.J., 2008. C_{60} colloid formation in aqueous systems: effects of preparation method on size, structure, and surface, charge. *Environmental Science & Technology*, **42**(1):173-178. [doi:10.1021/es071248s]

Hwang, Y.S., Li, Q.L., 2010. Characterizing photochemical transformation of aqueous nC_{60} under environmentally relevant conditions. *Environmental Science & Technology*, **44**(8):3008-3013. [doi:10.1021/es903713j]

Hyung, H., Kim, J.H., 2009. Dispersion of C_{60} in natural water and removal by conventional drinking water treatment processes. *Water Research*, **43**(9):2463-2470. [doi:10.1016/j.watres.2009.03.011]

Isaacson, C.W., Bouchard, D.C., 2010. Effects of humic acid and sunlight on the generation and aggregation state of aqu/C_{60} nanoparticles. *Environmental Science & Technology*, **44**(23):8971-8976. [doi:10.1021/es103029k]

Kim, K., Jang, M., Kim, J., *et al*., 2010. Effect of preparation methods on toxicity of fullerene water suspensions to Japanese medaka embryos. *Science of The Total Environment*, **408**(22):5606-5612. [doi:10.1016/j.scitotenv.2010.07.055]

Kim, K.T., Jang, M.H., Kim, J.Y., *et al*., 2012. Embryonic toxicity changes of organic nanomaterials in the presence of natural organic matter. *Science of The Total Environment*, **426**:423-429. [doi:10.1016/j.scitotenv.2012.03.050]

Li, M.H., Huang, C.P., 2010. Stability of oxidized single-walled carbon nanotubes in the presence of simple electrolytes and humic acid. *Carbon*, **48**(15):4527-4534. [doi:10.1016/j.carbon.2010.08.032]

Li, Q.L., Xie, B., Wang, Y.S., *et al*., 2009. Kinetics of C_{60} fullerene dispersion in water enhanced by natural organic matter and sunlight. *Environmental Science & Technology*, **43**(10):3574-3579. [doi:10.1021/es803603x]

Lin, D.H., Liu, N., Yang, K., *et al*., 2009. The effect of ionic strength and pH on the stability of tannic acid-facilitated carbon nanotube suspensions. *Carbon*, **47**(12):2875-2882. [doi:10.1016/j.carbon.2009.06.036]

Lin, D.H., Liu, N., Yang, K., *et al*., 2010. Different stabilities of multiwalled carbon nanotubes in fresh surface water samples. *Environmental Pollution*, **158**(5):1270-1274. [doi:10.1016/j.envpol.2010.01.020]

Lin, D.H., Li, T.T., Yang, K., *et al*., 2012a. The relationship between humic acid (HA) adsorption on and stabilizing multiwalled carbon nanotubes (MWNTs) in water: effects of HA, MWNT and solution properties. *Journal of Hazardous Materials*, **241-242**:404-410. [doi:10.1016/j.jhazmat.2012.09.060]

Lin, D.H., Tian, X.L., Li, T.T., *et al*., 2012b. Surface-bound humic acid increased Pb^{2+} sorption on carbon nanotubes. *Environmental Pollution*, **167**:138-147. [doi:10.1016/j.envpol.2012.03.044]

Mashayekhi, H., Ghosh, S., Du, P., *et al*., 2012. Effect of natural organic matter on aggregation behavior of C_{60} fullerene in water. *Journal of Colloid and Interface Science*, **374**(1):111-117. [doi:10.1016/j.jcis.2012.01.061]

Nakamura, E., Isobe, H., 2003. Functionalized fullerenes in water. The first 10 years of their chemistry, biology, and nanoscience. *Accounts of Chemical Research*, **36**(11):807-815. [doi:10.1021/ar030027y]

Navarro, D.A., Kookana, R.S., Kirby, J.K., *et al*., 2013. Behaviour of fullerenes (C_{60}) in the terrestrial environment: potential release from biosolids-amended soils. *Journal of Hazardous Materials*, **262**:496-503. [doi:10.1016/j.jhazmat.2013.08.021]

Nel, A., Xia, T., Madler, L., *et al*., 2006. Toxic potential of materials at the nanolevel. *Science*, **311**(5761):622-627. [doi:10.1126/science.1114397]

Oberdörster, E., Zhu S.Q., Blickley, T.M., *et al*., 2006. Ecotoxicology of carbon-based engineered nanoparticles: effects of fullerene (C_{60}) on aquatic organisms. *Carbon*, **44**(6):1112-1120. [doi:10.1016/j.carbon.2005.11.008]

Qu, X.L, Hwang, Y.S., Alvarez, P.J., *et al*., 2010. UV irradiation and humic acid mediate aggregation of aqueous fullerene (nC_{60}) nanoparticles. *Environmental Science & Technology*, **44**(20):7821-7826. [doi:10.1021/es101947f]

Takada, H., Kokubo, K., Matsubayashi, K., *et al*., 2006. Antioxidant activity of supramolecular water-soluble fullerene evaluated by β-carotene bleachingassay. *Bioscience, Biotechnology, and Biochemistry*, **70**(12):3088-3093. [doi:10.1271/bbb.60491]

Tian, X.L., Zhou, S., He, X., *et al*., 2010. Metal impurities dominate the sorption of a commercially available carbon nanotube for Pb(II) from water. *Environmental Science & Technology*, **44**(21):8144-8149. [doi:10.1021/es102156u]

van Wezel, A.P., Moriniere, V., Emke, E., *et al*., 2011. Quantifying summed fullerene nC_{60} and related transformation products in water using LC LTQ Orbitrap MS and application to environmental samples. *Environment International*, **37**(6):1063-1067. [doi:10.1016/j.envint.2011.03.020]

Xie, B., Xu, Z.H., Guo, W.H., *et al*., 2008. Impact of natural organic matter on the physicochemical properties of aqueous C_{60} nanoparticles. *Environmental Science & Technology*, **42**(8):2853-2859. [doi:10.1021/es702231g]

Yang, Y.K., Nakada, N., Nakajima, R., *et al*., 2013. pH, ionic strength and dissolved organic matter alter aggregation of fullerene C_{60} nanoparticles suspensions in wastewater. *Journal of Hazardous Materials*, **244-245**:582-587. [doi:10.1016/j.jhazmat.2012.10.056]

Zhang, W., Rattanaudompol, U., Li, H., *et al*., 2013. Effects of humic and fulvic acids on aggregation of aqu/nC_{60} nanoparticles. *Water Research*, **47**(5):1793-1802. [doi:10.1016/j.watres.2012.12.037]

中文概要：

本文题目：腐殖酸对富勒烯 C_{60} 的悬浮作用

The role of humic acid in stabilizing fullerene (C_{60}) suspensions

研究目的：腐殖酸（HA）对富勒烯（C_{60}）粉末的悬浮作用以及 pH、离子强度对 HA-C_{60} 悬浮性能的影响。

创新要点：研究水质条件对 C_{60} 悬浮性能的影响。

研究方法：测定 C_{60} 粉末在 HA 溶液中的 zeta 电位，水力学粒径和悬浮浓度；HA 存在下，C_{60} 悬浮体系的 zeta 电位与水力学粒径随 pH 的变化及 C_{60} 悬浮体系团聚动力学随离子强度的变化。

重要结论：HA 对 C_{60} 粉末起到一定的分散作用，但不能使其长时间稳定悬浮于水中。当 pH<4 时，C_{60} 水悬液开始沉淀；而当 HA 存在时，C_{60} 水悬液在 pH 3–11 范围内都保持稳定，这是由于 HA 吸附于 C_{60} 表面，通过静电排斥和空间位阻作用，促进 C_{60} 分散悬浮。C_{60} 水悬液的稳定性随盐离子价位和浓度升高而降低。HA 会抑制 Na^{+} 对 C_{60} 水悬液的脱稳作用；但高价离子 Ca^{2+} 和 La^{3+} 存在时，HA 与 C_{60} 之间会发生桥联从而促进 C_{60} 水悬液脱稳沉淀。

关键词组：富勒烯；腐殖酸；胶体稳定性；天然有机质；纳米材料